

Proceedings of the Korean Nuclear Society Spring Meeting
Cheju, Korea, May 2001

Current Status and Activities on the Pohang Neutron Facility

G. N. Kim, D. Son

Center for High Energy Physics, Kyungpook National University, Taegu 702-701, Korea

Y. S. Lee, V. Kovalchuk⁺, V. Skoy*, M. H. Cho, I. S. Ko, W. Namkung
Pohang Accelerator Laboratory, Pohang University of Science and Technology,
Pohang 790-784, Korea

D. W. Lee, H. D. Kim

Physics Department, Pusan National University, Pusan 609-749, Korea

S. K. Ko

Physics Department, University of Ulsan, Ulsan 680-749, Korea

D. S. Kim

Physics Education Department, Taegu University, Kyungbuk 712-714, Korea

T. I. Ro, Y. G. Min

Physics Department, Donga University, Pusan 604-714, Korea

Abstract

The Pohang Neutron Facility, an electron linear accelerator based pulsed neutron facility, was constructed for nuclear data production in Korea. It consists of an electron linear accelerator, a water-cooled Ta target with a water moderator, and a time-of-flight path with an 11 m length. The neutron energy spectra are measured for different water levels inside the moderator and compared with calculations by the Monte Carlo N-Particle (MCNP) transport code. The optimum size of the water moderator is determined on the base of these results.

⁺ Permanent address: Troitsk Institute for Innovation and Thermonuclear Research, Moscow, Russia

* Permanent address: Frank Laboratory of Neutron Physics, JINR, Dubna, Russia

1. Introduction

Among the various kinds of neutron sources (reactors, accelerator-based neutrons, and radioisotopic neutron emitters), the accelerator-based neutron source is the most efficient one for high-resolution measurements of microscopic neutron cross sections. It produces short bursts of neutrons with a broad continuous energy spectrum by nuclear reactions of energetic photons or charged particles. Especially, an electron linear accelerator (linac) is a powerful tool to produce intense pulsed neutrons. Pulsed neutrons based on an electron linac are effective for measuring energy dependent cross sections with high resolution by the time-of-flight (TOF) technique covering the energy range from thermal neutrons to a few tens of MeV. The measurement of neutron cross sections gives basic information for the study of neutron interactions with nuclei. Precise measurements of neutron cross sections are of great importance for the safety design of nuclear reactors and for the evaluation of the neutron flux density and energy spectrum around a reactor.

A nuclear data project was initiated to construct infrastructures for nuclear data at the Korea Atomic Energy Research Institute (KAERI). There was little activity for nuclear data production experiment until this project was launched. Since then, the collaboration group for nuclear data production was organized from several universities in Korea. The pulsed neutron facility using an electron linac was proposed in 1997 at the Pohang Accelerator Laboratory (PAL) [1]. The electron linac was designed and constructed based on experiences obtained from construction and operation of the 2-GeV electron linac at PAL [2]. The nominal beam energy of the designed electron linac was 100 MeV with RF power of 80 MW, and the operating frequency was 2,856 MHz.

The neutron energy spectra are measured for different water levels inside the moderator and compared with the calculation results by the Monte Carlo N-Particle (MCNP) transport code system [3]. The optimum size of the water moderator is determined on the base of these results.

2. Pohang Neutron Facility

The Pohang Neutron Facility (PNF) consists of an electron linac, a water-cooled Ta target, and an 11 m long TOF path. The electron linac consists of a thermionic RF-gun, an alpha magnet, four quadrupole magnets, two SLAC-type accelerating sections, a quadrupole triplet, and a beam-analyzing magnet. A 2-m long drift space is added between the first and the second accelerating section to insert an energy compensation

magnet or a beam transport magnet for other research. The overall length of the linac is about 15 m. The RF-gun is one cell cavity with a dispenser cathode of 6 mm diameter. The RF-gun produces electron beams of 1 MeV, 300 mA, and 1.5 μ s [4]. The alpha magnet is used to match the longitudinal acceptance from the gun to the first accelerating section. Electrons move along an alpha-shaped trajectory in the alpha magnet with the bend angle of 278.6°. Four quadrupole magnets are used to focus the electron beam in the beam transport line from the thermionic RF-gun to the first accelerating section. The quadrupole triplet installed between the first and the second accelerating sections is used to focus the electron beam during the transport to the experimental beam line at the end of the linac.

After the RF-conditioning of the accelerating structures and the wave-guide network, we tested the beam acceleration [5]. The available RF power from a SLAC 5045 klystron was up to 45 MW due to the peak power limitation of the existing pulse modulator. The RF power fed to the RF-gun was 3 MW. The beam energy is 75 MeV, and the measured beam currents at the entrance of the first accelerating structure and at the end of the linac are 100 mA and 40 mA, respectively. The length of electron beam pulses is 1.5 μ s, and the pulse repetition rate is 12 Hz. The diameter of electron beam is about 20 mm at the beam profile monitor in front of the target. The measured energy spread is about 1~3 %. The energy spread was reduced by adjustment of the RF phase for the RF-gun and by optimization of the magnetic field for the alpha magnet.

As a photoneutron target, it is necessary to use heavy mass materials in order to produce intense neutrons by way of bremsstrahlung under high-power electron beams. We have chosen a tantalum as the target material, which has advantages of high density (16.6 g/cm³), high melting point (3,017°C), and high resistant against the corrosion by cooling water.

Since we have to utilize the space and infrastructures at PAL, an 11 m long TOF path and a detector room were constructed vertically to the electron linac. The TOF tubes were made by stainless steel with two different diameters of 15 and 20 cm.

3. Experimental Arrangement

The experimental setup for the neutron TOF spectrum measurement is shown in Fig. 1. The Ta target is located at a position where the electron beam hits the target center, and the target is aligned vertically with the center of the TOF tube. A water-cooled Ta target was designed by the Electron Gamma Shower simulation code, EGS4 [6]. The Ta target as shown in Fig. 2 was composed of ten Ta sheets, 49 mm in diameter

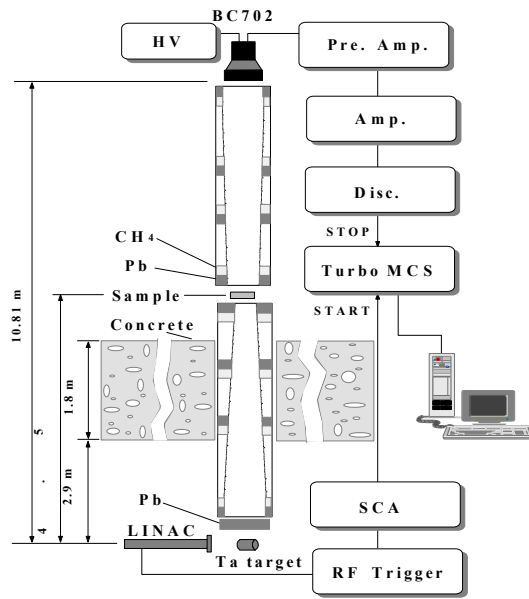


Fig.1. Experimental setup and a block diagram for data acquisition.

and 74 mm in total length [7]. There was 1.5 mm water gap between Ta sheets in order to cool the target effectively. The target housing was made of 0.5 mm thick titanium. The calculated conversion ratio from a 100 MeV electron to neutrons was 0.032 obtained by using the EGS4. According to this result, the neutron yield per kW beam power for the electron energy above 40 MeV at the target was 2.0×10^{12} n/sec, which was about 2.5% lower than the calculated value based on the Swanson's formula, $1.21 \times 10^{11} Z^{0.66}$, where Z is the atomic number of the target material and the electron energy is above 40 MeV [8].

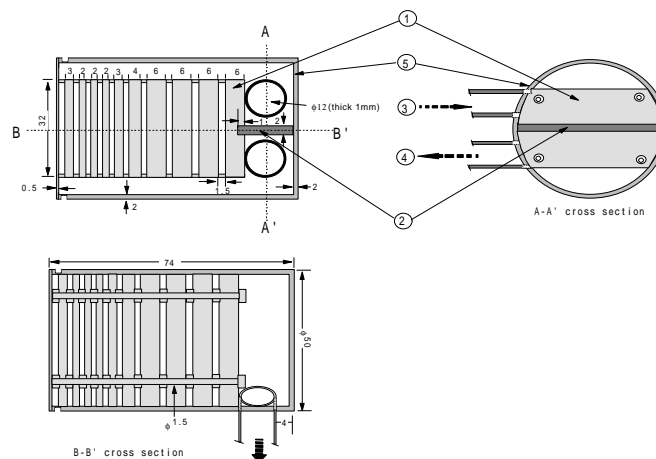


Fig.2. Schematics of the water-cooled Ta target: Ta plate, Parting strip, Cooling water(inlet), Cooling water(outlet), Ti housing. The numbers refer to dimensions in mm.

This target was set at the center of a water moderator made by using an aluminum cylinder with a thickness of 0.5 cm, a diameter of 30 cm and a height of 30 cm. The water moderator was mounted on an aluminum plate with a thickness of 2.5 cm and an iron table with a thickness of 2 cm as shown in Fig. 3. The rear part of the water moderator is covered by a 10 cm thick lead.

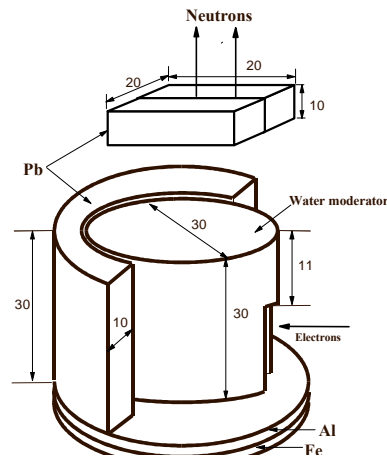


Fig.3. Geometry shows the target system used in the experiment and MCNP calculation.

A Pb block, 20 cm \times 20 cm in area by 10 cm in thickness, was placed at the entrance of 15 cm diameter TOF tube to reduce the gamma flash generated by the electron burst from the target and scattered high-energy neutrons. In addition, a 0.5 cm thick Pb plate was attached in front of the TOF tube. Lead was chosen due to its low energy cross section which is about 3 barns at 0.007 eV and 11 barns above 0.2 eV; therefore the lead block can serve as an effective low band filter removing more fast neutrons than sub-thermal neutrons. There is 1.8 m thick concrete between the target room and the detector room. The sample was placed at the midpoint of the TOF path.

As a neutron detector, we used a $^6\text{Li-ZnS(Ag)}$ scintillator BC702 with a diameter of 12.5 cm and a thickness of 1.5 cm mounted on an EMI-93090 photomultiplier. It was located at a distance of 10.8 m from the photoneutron target. The neutron detector was shielded by lead bricks and borated polyethylene plates.

In order to monitor the neutron intensity during the experiment, a BF_3 proportional counter with a diameter of 1.6 cm and a length of 5.8 cm was placed in the target room at a distance of about 6 m from the target. The BF_3 counter was inserted in a polyethylene sphere with a diameter of 30.5 cm and surrounded by borated polyethylene with a thickness of 5 cm and Pb bricks with a thickness of 10 cm to shield thermal neutrons generated from the moderator and walls inside the target room and to protect gamma flash generated by the electron burst from the target. The neutron detector with

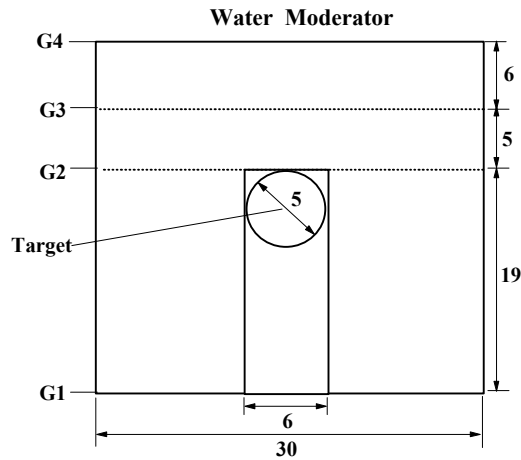


Fig.4. The geometry used in MCNP for optimizing the water level: G1, G2, G3, and G4 indicate the water level in the moderator vessel. The numbers refer to dimensions in cm.

a polyethylene sphere has a good response for fast neutrons [9].

In order to investigate the neutron energy spectra for the different water levels in the moderator, we used four water levels as shown in Fig. 4. G1 represents the geometry without water inside the moderator. G2 corresponds to 0 cm water level above the target in which water is around the target but no water above the target. G3 is the geometry with a water level of 5 cm above the target surface. Geometry G4 is a full of water in the moderator, which corresponds to 11 cm water level from the target surface. The cooling water inside the Ta target could not change significantly the spectral distribution of original photoneutrons.

4. Data Acquisition

The neutron energy spectra produced from a tantalum target with a water moderator were measured by the TOF method. As shown in Fig. 2, the TOF signal from a ${}^6\text{Li-ZnS(Ag)}$ scintillator was connected to an amplifier system (ORTEC-113 pre-amplifier and ORTEC-571 amplifier). The amplifier output was then fed a discriminator (Disc.) input, whose output was used as a stop signal of a 150 MHz time-digitizer (Turbo MCS). The lower threshold level of the discriminator was set to 30 mV. The Turbo MCS was operated as a 16384-channel time analyzer. The channel width of the time analyzer was set to 0.5 μs . The 12 Hz trigger signal (RF Trigger) for the modulator of the electron linac was connected to an ORTEC-550 single channel analyzer (SCA), the output signal was used as the start signal for the Turbo MCS. The Turbo MCS is connected to a

personal computer. The data were collected, stored and analyzed on this computer.

The block diagram of the data acquisition system for the BF_3 neutron monitor in the

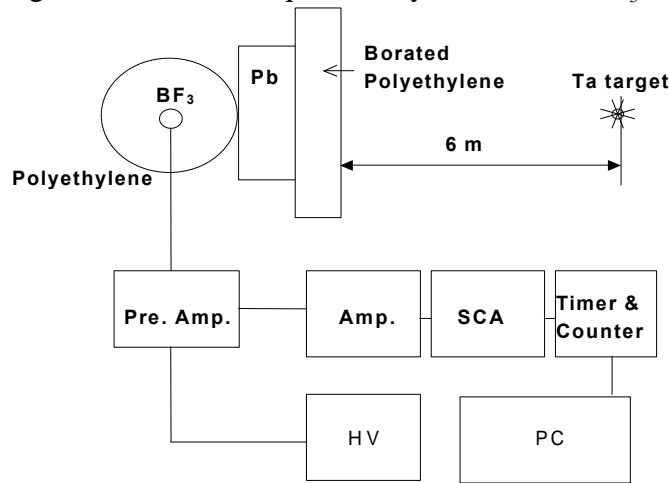


Fig.5. Experimental arrangement for a BF_3 neutron monitor in the target room and block diagram for data acquisition.

target room is shown in Fig. 5. The signal from a BF_3 counter was connected to an ORTEC-590A spectrometric amplifier (Amp.) through an ORTEC-142PC preamplifier (Pre. Amp.). The amplifier output was fed to an ORTEC-SCA550 single channel analyzer (SCA). The single channel analyzer was used to create the standard signal and to cut noises originating from gamma rays and low-energy neutrons. The output signal from the single channel analyzer was fed into an ORTEC-996 timer and counter. The counter was connected to a personal computer.

During the experiment, the electron linac was operated with a repetition rate of 12 Hz, a pulse width of $1.5 \mu\text{s}$, a peak current of 30 mA, and electron energy of 60 MeV.

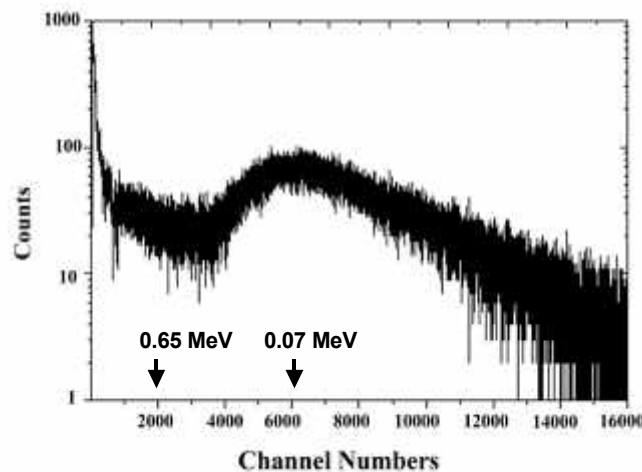


Fig.6. Typical neutron spectrum for the G3 geometry measured at 11-m TOF path length.

5. Data Analysis

The neutron energy spectra generated by the Ta target with a water moderator with different water levels of G1-G4 were measured with the TOF method at PNF. Fig. 6 shows a typical neutron TOF spectrum for the G3 geometry. The neutron energy spectrum mainly consists of fast neutrons and thermal neutrons produced in the water moderator and scattered neutrons from the wall and other materials around the target. The TOF spectrum was only measured in the direction perpendicular to the incident electron beam. In order to estimate the background level, we took neutron TOF spectra for a Sm sample with a Cd filter of 0.5 mm in thickness and a run without any samples (blank run). The background level was estimated from the fitting function

$$F(I) = a + b \times I + c \times I^2 \quad (1)$$

where a , b , and c are constants and I is the channel number of the time digitizer in Fig. 7. The resonances in the neutron TOF spectrum for the blank run are related to Sb and W impurities inside the Pb block. The signal-to-background ratio defined as the neutron counts minus background counts divided by the background counts at a

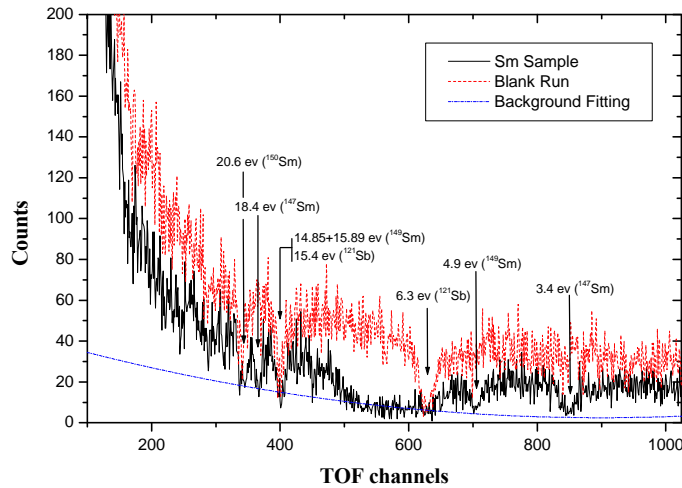


Fig.7. Typical background level is measured at 11-m TOF path length. Solid line and dotted line represent the TOF spectrum for Sm sample and without any sample in the beam line, respectively.

particular energy was about 10 to 1.

5. 1 Neutron Monitor Counts

The BF_3 neutron monitor in the target room was operated in the count mode as a neutron monitor. The neutron monitor was tested by using a neutron source ^{252}Cf with a mean neutron energy of 2.13 MeV and an activity of 5.4×10^4 n/sec. The pulse shape of the neutron monitor was checked with an oscilloscope and no saturation was observed

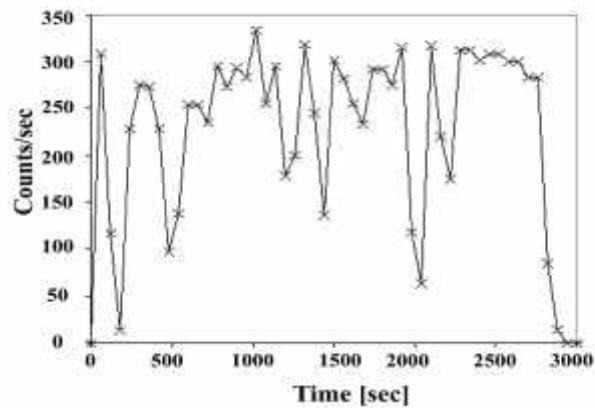


Fig.8. Typical neutron intensity measured by a BF_3 monitor for an hour operation.

during the linac pulse duration. The typical behavior of neutron counts during one period of experiment is shown in Fig. 8. Neutron counts during the experiment were changed due to the unstable modulator system for the electron linac. The typical count rate of the neutron monitor was about 300 counts per second except for several points, which were due to the trips in the pulse modulator system. The total counts in the neutron monitor were used to normalize the neutron intensity between the runs. The background count rates were measured before and immediately after operating the accelerator. The background count rates for the BF_3 neutron monitor were less than 0.01 counts per second.

5.2 Neutron Energy Spectrum

The measured TOF spectra as a function of the channel number were normalized using the neutron counts from the neutron monitor and converted as a function of neutron energy. Each channel I in the time analyzer is converted to the

neutron energy E_i via:

$$E_i = \left\{ \frac{72.3 \times L}{(I - I_0) \times \Delta t} \right\}^2 \quad (2)$$

where L is the neutron flight path in meters, Δt is the channel width in μs and set to $0.5 \mu s$, and I_0 is the number of channel at the time of flight equals to zero when the neutron burst was produced. The relation between a channel number of the neutron TOF spectrum and its energy was calibrated with resonance energies of Ta, Sm, and other samples with a black resonance. Good linearity was found between the neutron TOF and the channel number. We found the flight path length L equal to 10.81 ± 0.02 m.

The measured neutron flux was corrected for the detector efficiency, $e(E_i)$ which is energy dependent and is given by:

$$e(E_i) = 1 - \exp\left(-\frac{t}{C\sqrt{E_i}}\right) \quad (3)$$

where t is the thickness of scintillator in centimeters and C is a constant for each scintillator and is given by the manufacturer [10]. We used $C = 12.5 \text{ cm/eV}^{0.5}$ for a BC702 ${}^6\text{Li-ZnS(Ag)}$ scintillator.

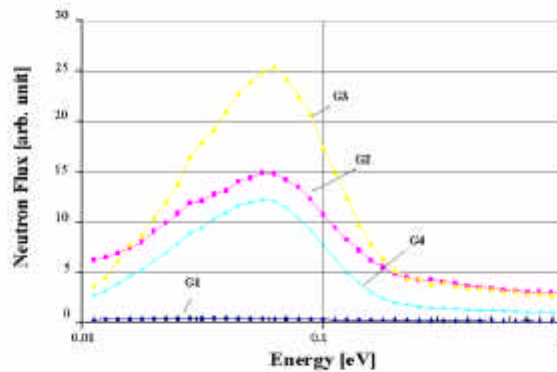


Fig.9. Measured neutron flux for different geometry in the neutron energy from 0.01 to 1 eV. G1 to G4 correspond to the geometry shown in Fig.4.

Figure 9 shows the neutron flux (number of neutrons per energy group) in the energy range of 0.01 to 1 eV for different water levels. The neutron flux in each channel was summed up over every 0.23 lethargy width. The G3 geometry with a water level of 5 cm gives more thermal neutrons compared to other geometries. Too high water level in the moderator decreases thermal neutrons due to the absorption of thermal neutrons.

5.3 Comparison with MCNP calculation

The continuous energy Monte Carlo code MCNP version 4B has been used to calculate the neutron spectra for various geometries. The MCNP code has its own nuclear data library generated from the evaluated nuclear data files of ENDF/B-VI [11]. Using the MCNP statistical sampling technique, the neutron distributions of moderated neutrons were calculated as a function of time and energy. The purpose of this calculation is to compare them with measurements for the thermal neutron flux leaving the water moderator and to optimize the photoneutron target system.

The neutron source term for the tantalum plates in the target was chosen to be an “evaporation” energy spectrum [12, 13] given by

$$f(E) = cE \exp(-E/T) \quad (4)$$

where E is the neutron energy in MeV, T is the effective temperature of the tantalum target in MeV, and $c=4.7259$ is a normalization constant. Using an effective temperature of 0.46 MeV [14], Eq. (4) gives the average neutron energy about 0.92 MeV. The source parameters were chosen such that the neutrons at “birth” are distributed uniformly throughout a homogenized mixture of tantalum and cooling water with an isotropic angular distribution [15].

In the calculation, we ignore the effect of aluminum wall of the water moderator because of its small contribution to the total flux of scattered neutrons. The minimum and maximum neutron cutoff energies were 0.0001 eV and 10 MeV, respectively. The neutron time cutoff was 10^7 Shakes (1 Shake = 10^{-8} sec). The energy region was divided into 200 groups with an equal lethargy width. The number of particle history was 50,000,000 counts per each geometry. The neutron current was calculated within 15 degrees with respect to the line connecting from the center of the target to the detector for different water levels inside the moderator.

Figure 10 shows the neutron flux calculated by MCNP code for different geometries described above. For fast neutrons in the energy regions of 0.1 to 10 MeV, the neutron

flux for geometry G1 and G2 is almost the same and higher than other geometry

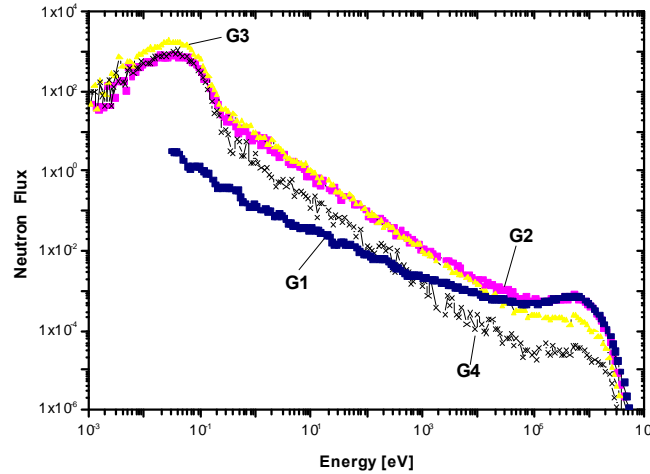


Fig.10. Neutron energy spectra in the water moderator calculated by the MCNP code for different geometry as shown in Fig.4.

because there is no water above the target surface. Based on this calculation, the neutron flux in the energy bin of 0.01 to 0.1 eV as a function of water height were normalized and plotted in Fig. 11. The points correspond to MCNP calculations and the line is a polynomial spline interpolation.

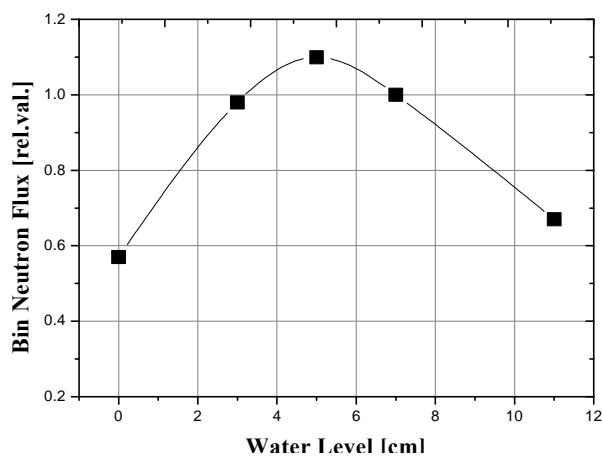


Fig.11. Calculated neutron flux is given as a function of the water level in the moderator in the neutron energy from 0.01 eV to 0.1 eV. The measured points are connected by a spline fit. In this figure, 0, 5 and 11 cm correspond to G2, G3, and G4 geometries, respectively.

In this figure, 0, 5, and 11 cm of water level correspond to G2, G3, and G4 geometries, respectively. The water height for the maximum neutron flux was found to be about 5 cm, which corresponds to geometry G3. This is in good agreement with Kiyangi's experimental results that found an optimum thickness of 5.5 cm for a 25 cm × 25 cm × 5.5 cm water moderator [16] and with also our measurement as shown in Fig. 9.

The measured differential neutron flux for three geometries were shown in Fig. 12 compared with those of the MCNP calculations. In this figure, the neutron flux for G3 (G4) geometry was multiplied with a factor 10 (0.1) for better visualization. The points (squares, triangles, and circles are for G2, G3, and G4 geometry, respectively) represent the result of the MCNP calculation. The measured energy spectra were normalized using the neutron monitor counts. The calculated spectra have relative normalization (normalization coefficients are C1= 3540 for G2, C2=35400 for G3, and C3=354 for G4). The measured neutron spectra were well agreed with those of the MCNP calculation within the experimental uncertainty. The statistical uncertainty of MCNP calculation was ranged from 3 to 9 % depending on the energy bin.

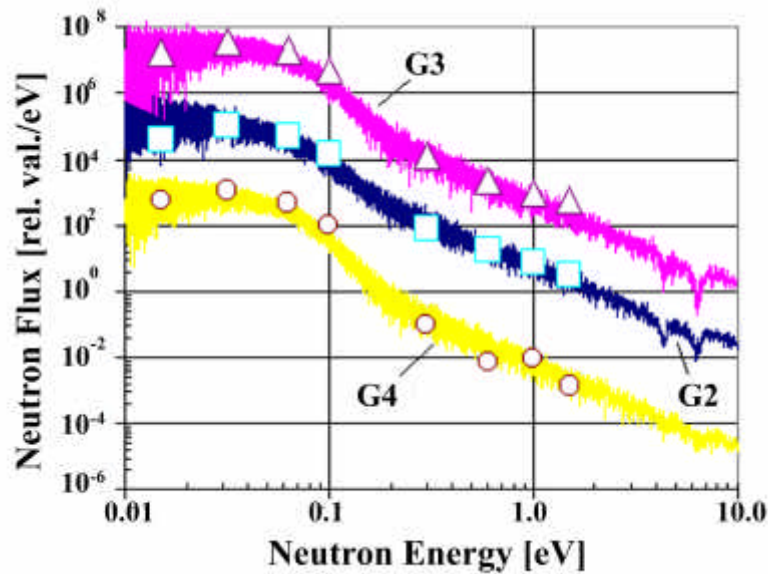


Fig.12. Measured and calculated neutron fluxes are given for three different geometries. The points correspond to MCNP calculation and the spectrum for G3 (G4) geometry is multiplied by a factor 10 (0.1) for better view.

6. Conclusion

In order to construct infrastructures for nuclear data production, the Pohang Neutron Facility based on an electron linac was constructed in December 1999. From March 2000, the electron linac was operated with a repetition rate of 12 Hz, a pulse width of 1.5 μ s, a peak current of 30 mA, and an electron energy of 60 MeV in order to test a target system, a data acquisition system, and measure the neutron energy spectrum. The neutron energy spectra produced by the photoneutron target with a water moderator were measured with a ${}^6\text{Li-ZnS(Ag)}$ glass scintillator as a neutron detector with the neutron TOF method at 11 m flight path of the Pohang Neutron Facility. As a neutron monitor, a BF_3 proportional counter was used. The neutron TOF spectra were normalized with the total counts in the neutron monitor. We measured the neutron TOF spectra for different water levels inside the moderator and compared experimental results with the MCNP calculations in order to maximize the thermal neutron flux.

The measured neutron energy spectra for different water levels in the moderator were verified by the MCNP calculations. The experimental and calculated data were well agreed within the experimental uncertainty. According to the results of the measurement and the calculation, the 5 cm water level in the moderator gives the maximal thermal neutron flux for the present geometry of the photoneutron target system.

Acknowledgement

The authors would like to express their sincere thanks to the staff of the Pohang Accelerator Laboratory for the excellent operation of an electron linac and strong support. This work is partly supported through the Long-Term Nuclear R&D program by the Korea Atomic Energy Research Institute.

References

- [1] G. N. Kim *et al.*, "Proposed Neutron Facility using 100-MeV electron linac at Pohang Accelerator Laboratory," in Proc. International Conference on Nuclear Data for Science and Technology (Trieste, Italy, May 19-24, 1997), Edited by G. Reffo, A. Ventura and C. Grandi, 556 (1997).
- [2] J. Y. Cho *et al.*, "Design of 100-MeV electron Linac for Neutron Beam Facility at

- PAL,” in Proc. 1997 KAPRA Workshop (Seoul, Korea, June 26-27, 1997), Korea Accelerator and Plasma Research Association, 88 (1997).
- [3] MCNP, “A General Monte Carlo N-Particle Transport Code System, Version 4B”, Los Alamos National Laboratory, LA-12625-M (1997).
- [4] H. S. Kang, G. N. Kim, M. H. Cho, W. Namkung, and K. H. Chung, IEEE Trans. Nucl. Sci. **44** (1997), 1639.
- [5] H. S. Kang *et al.*, “Beam Acceleration Result of Test Linac,” in Proc. First Asian Particle Accelerator Conference (Tsukuba, Japan, Mar. 23-27, 1998), Edited by Y. H. Chin *et al.*, 743 (1998).
- [6] W. R. Nelson, H. Hirayama and D. W. O. Rogers, “The EGS4 Code System,” SLAC Report 265 (1985).
- [7] W. Y. Baek *et al.*, “Design of the Photoneutron Target for Pulsed Neutron Sources at PAL,” in Proc. Workshop on Nuclear Data Production and Evaluation (Pohang, Korea, Aug. 7-8, 1998), Edited by J. Chang and G. N. Kim, KAERI/GP-130/98 (1998).
- [8] W. P. Swanson, “Radiological Safety Aspects of the Operation of Electron Linear Accelerators,” IAEA Technical Reports No. 188 (1979).
- [9] V. Mares and H. Schrauble, Nucl. Instr. and Meth. A 337 (1994) 461; V. Mares and H. Schrauble, Nucl. Instr. and Meth. A **366** (1995), 203.
- [10] Scintillation detector. BC702. Bicron. Saint-Gobain Norton Industrial Ceramics Inc., User’s Manual, USA (1997).
- [11] ENDF/B-VI, “Evaluated Nuclear Data Files,” Brookhaven National Laboratory, National Nuclear Data Center, On-line data service (1997).
- [12] Y. Danon, “Design and construction of the RPI enhanced thermal neutron target and thermal cross section measurements of rare earth isotopes,” Doctoral Thesis, Rensselaer Polytechnic Institute (1993).
- [13] Y. Danon, R. C. Block, R. E. Slovacek, Nucl. Instr. and Meth. A **352** (1995) 596.
- [14] C. R. Stopa, “Measurements of neutron induced fission cross sections of ^{244}Cm , ^{246}Cm and ^{248}Cm by means of lead slowing-down-time spectrometry,” Doctoral Thesis, Rensselaer Polytechnic Institute (1983).
- [15] M. E. Overberg, B. Moretti, R. Slovacek, R. Block, Nucl. Instr. and Meth. A **438** (1999), 256.
- [16] Y. Kiyonagi, J. of Nucl. Sci. Technol. **19** (1982), 352.